Scholar Publishing Group
International Journal of Big Data Intelligent Technology
https://doi.org/10.38007/IJBDIT.2020.010206
ISSN 2790-0932 Vol. 1, Issue 2: 74-90

Sem Image Based on Denoising Algorithm Shows the Effect of PTO Seed Layer on the Crystallization Temperature and Electrical Properties of PZT Ferroelectric Thin Films

Romanya Vijue*

New Valley University, Egypt

**corresponding author*

Keywords: Denoising Algorithm, Sem Image, PTO Seed Layer, PZT Ferroelectric Film Crystallization Temperature, Electrical Properties

Abstract: Lead zirconate titanate (PZT) materials have been widely studied because of their excellent dielectric, ferroelectric, piezoelectric and electro-optic effects.The electrical properties of ferroelectric thin films indicate that the temperature of ferroelectric thin films changes under the action of external light field under adiabatic conditions. Previous studies have shown that the crystal orientation of ferroelectric films is an important factor affecting the local structure of ferroelectric films. Therefore, starting from the micro domain structure, the effects of denoising algorithm on the crystallization temperature and electrical properties of PZT ferroelectric thin films shown in SEM were studied. At the same time, the crystalline layers in the microstructure of PZT and PZT / PTO films were analyzed by SEM images, and the electrical properties of PZT films were compared with ferroelectric and stable dielectric properties. The experimental results show that the residual polarization intensity obtained by annealing at $550^{o}C$ after adding PTO seed layer is about $20\mu C/cm^{2}$, which is basically the same as that obtained by annealing PZT ferroelectric film at $650^{o}C$. Therefore, the ferroelectric properties of PZT film are enhanced after adding PTO seed layer. Moreover, the dielectric loss of PZT / PTO film is smaller than that of PZT film.

1. Introduction

1.1. Background

With the rapid development of information technology, there are more and more media for

information communication, mainly including text, image, sound and so on. Among many sources of information, the channel for human to obtain information mainly comes from images. The image is easily disturbed by some noise in the process of acquisition, sampling, transmission and coding. The existence of noise changes the gray value of pixels, resulting in the misleading of external information in the reading process. Therefore, in order to obtain an image without noise interference, it is necessary to denoise the noisy image. In recent years, with the continuous research and improvement of image filtering algorithms by researchers, many new denoising algorithms have been proposed, and the denoising algorithm processing of SEM image presentation has gradually sprung up.

1.2. Significance

Ferroelectric materials are widely used in memory, thin film capacitors, piezoelectric sensors, infrared detection and acousto-optic deflectors because of their good ferroelectric, dielectric, pyroelectric, piezoelectric and other electro-optic effects. However, PZT ferroelectric thin film materials still have some shortcomings in some electrical properties, so it needs to be further studied.

1.3. Related Work

Scanning electron microscope image analysis is an interesting option for inertial analysis of nanostructure properties. The algorithm based on convolutional neural network (CNN) improves the estimation of scanning electron microscope (SEM) image noise and linear roughness measurement. However, these algorithms must evolve to run at high speed with low memory without normal damage. Chaudhary n introduces two ways to reduce time and memory. He first proposed depth CNN linenet1 and linenet2 to construct and calculate the edges of SEM images at the same time. Multiple functional concepts in linenet1 and linenet2 reduce training time, reference time and model size. Linenet2 also promotes edge compression in multiline graphs and combines other geometric methods. His training method uses single line scanning electron, linear MICROSCAN electron and systematic ear position information to train the data system. Next, we will look at different visualization tools to improve your understanding. Therefore, the research content needs to be further improved [1]. Because the SnO 2 membrane (PTO) impregnated with PTO was prepared by immersion gel gel method. Huang x received X-ray diffraction (XRD), electron microscope (SEM), four point detector and UV-Vis spectrophotometer. The results show that the square rutile system is introduced into the PTO film under all test conditions. The square length of PTO film first decreases and then increases with the increase of phosphorus doping was annealing temperature and coating conditions. With the increase of annealing temperature, the surface length and grain compression increase. When the P / SN ratio is 2mol%, the annealing temperature is 450 ℃ and the number of coatings is 14 ℃, the optimal thin-layer resistance of PTO film is 8.9K Ω, and the transparency of visible light region is 95%, but it has not been applied [2]. Scientists' enthusiasm for ferroelectric materials has not weakened. The platinum ion film (100 nm) prepared by Basu n using the optimized reactive ion release mechanism shows p-type semiconductor behavior, with a side gap of 1.5ev, a resistivity of 0.16 Ω - M and a working power of 0.22ev. XPS spectrum shows the world of PTO phase (32%) and PtO2 phase (68%). XRD spectrum reflects α- Installation of PtO2 phase. A simple two terminal sensor image is made on a transparent and flexible acetate base plate. The platinum oxide film forms an active layer (8.0 mm x 60) m) for DNA detection. The working

principle of the sensor is that because DNA is attached to the surface of platinum material, the weight of the carrier changes, resulting in changes in behavior. The adhesion of DNA to platinum oxide was confirmed by Fourier transform infrared spectroscopy (FTIR) and optical fluorescence measurement. It can be found that for each percentage increase in fluorescence intensity, the stable absorption of DNA and platinum oxide is 7.35 μ m The sensor system displays the current channel according to the DNA concentration, but the test process is very complex [3]. We know that the absence of ferroelectric region in ferroelectric thin films will cause depolarization, resulting in the slope of lagging P (E) ring. Boettger u found that the depolarization factor is determined by the measured latency ratio of lead zirconate titanate (PZT) thin films, which contains a lot of information about the optical layer and the passive iron region in the body. The resulting interface capacity is less than that estimated by traditional extrapolation techniques. In addition, the concept of depolarization has been used to study the inhibition behavior of PZT films, indicating that the seed removal process leading to this phenomenon occurs in the whole film, but its effectiveness is very weak [4]. As the next generation of electronic equipment, visual and flexible electronic products have attracted much attention. In recent years, the application in specific environment (such as wind turbine) puts forward higher requirements for flexible equipment. Ren C uses pulsed laser technology to produce transparent Pb (zr0.1ti0.9) O-3 (PZT) on transparent indium tin (ITO) electrode on yttrium stabilized zirconia mica buffer.) Ferroelectric thin film. The characteristics, optical, mechanical and electronic properties of PZT / ITO / YSZ / oxide filament heterogeneity were studied. Heteroepitaxy has high transmissibility and excellent mechanical properties, and has excellent performance in rotation test. In addition, it also studies the electronic properties of PZT, which shows that PZT retains its original properties. Various calibration tests are performed to determine the ability of coordination function and confirm that the heterostructure maintains its physical properties under high temperature rotation. These results show that high-capacity flexible capacitors will pave the way for the application of flexible devices under harsh conditions, but the initial capital investment will be higher [5]. Thin film Pb (Zr < sub > 0.3 < / sub > Ti < sub > 0.7 < / sub >) O < sub > 3 < / sub > (PZT) is one of the most promising applications of nonvolatile ferroelectric random access memory (FRAM) because of its high residual polarization, rapid change behavior and process control preparation. Chen X uses sol-gel method to produce high quality PZT films with desired orientation and glossy appearance, and a piezoelectric operational microscope (PFM) is used to study the temperature dependence and local transformation behavior of ferroelectrics. Under the applied DC voltage, the domain structure system rotates 180 ° and is reconstructed. The hysteresis polarization analysis of PZT loop shows that as the temperature increases from 20 ℃ to 70 ℃, spontaneous polarization (P < sub > s < / sub >) and residual polarization (P < sub > R < / UB >) and voltage decrease (V < sub > C < / sub >) conform to the classical Landau phase transition process. In addition, PFM results show that PZT films always show good performance, which is very enlightening for our research [6].

1.4. Innovation

In the experiment of studying the influence of PZT ferroelectric film crystallization temperature and electrical properties, the SEM image of denoising algorithm is used to show the influence of PZT ferroelectric film crystallization temperature and electrical properties. In addition, PZT ferroelectric film with PTO seed layer is prepared, and the influence of PTO seed layer on PZT ferroelectric film crystallization temperature and electrical properties is studied and compared.

2. SEM Image Based on Denoising Algorithm Presents the Research Method of the Effect of Pto Seed Layer on the Crystallization Temperature and Electrical Properties of PZT Ferroelectric Thin Films

In real life, images are prone to noise pollution, but the degree of image damage needs to be judged. Observation through the human eye system is the smartest way to judge, but this way is easily disturbed by external factors and can not get the most accurate judgment. It is an effective method to judge the image quality according to the data and eliminate the influence of external factors. Evaluation criteria include sound evaluation criteria and self-evaluation criteria. Through the judgment of the two evaluation methods, the redundant results can be reduced and the objective data can be obtained. Therefore, these two judgment methods are generally used when calculating image quality.

2.1. Principle of Denoising Algorithm

With the increasing role of image information in human life, image processing becomes more and more important. Common field image denoising methods include spatial filtering and frequency domain filtering [7]. The common methods of spatial image denoising include mean filter, median filter and so on. Frequency domain filtering includes wavelet transform, Butterworth filtering, Gaussian filtering and so on. Several typical filtering algorithms are briefly introduced below.

(1) Mean filtering

As the name suggests, the mean value takes its average value. The working principle of mean filtering in image processing: the mean value of all pixels in the neighborhood centered on the current pixel replaces the gray value of the pixel [8], and its mathematical model can be expressed as:

$$z(i, j) = \frac{1}{PQ} \sum_{i=1}^{P} \sum_{j=1}^{Q} v(i, j) \tag{1}$$

Where, $z(i, j)$ represents the gray value of the filtered pixel, M and N respectively represent the number of rows and columns in the neighborhood of the pixel in the image, $v(i, j)$ represents the neighborhood of $P \times Q$ centered on (i, j) pixel in the image, and $P \times Q$ represents the number of pixel points in the neighborhood.

When different neighborhood sizes are used in the mean filtering algorithm, the noise processing effect will be different. In this paper, two mean filtering algorithms with different neighborhood sizes are used to filter the image containing Gaussian noise. The comparison of filtering effects is shown in Figure 1.

(a)Noise image (b)3*3 filtering effect (c)5 * 5 filtering effect

Figure 1. Denoising effect of mean filtering with different sizes

Looking at the comparison diagram of experimental results in Figure 1, we can see that there are great differences in noise phenomena when comparing algorithms with different local quantities. With the increase of area size, as edges and details become more and more important, the noise reduction effect is improved. Therefore, when using the mean filtering algorithm, selecting the appropriate area size is the key factor to improve the flow rate [9].

(2) Median filter

Intermediate filtering denoising process: the gray values of all pixels in the region are sorted by size, and the median value is used to replace the gray value of the space. The characteristics of median filter determine that the algorithm has good denoising effect on impulse noise. However, when the image has a large noise area, the selected median is also the particles polluted by noise, so the noise removal result is unsuccessful.

The comparison of processing results of median processing and mean processing in denoised image is shown in Figure 2. For comparison, the model of 5×5 treatment is used [10].

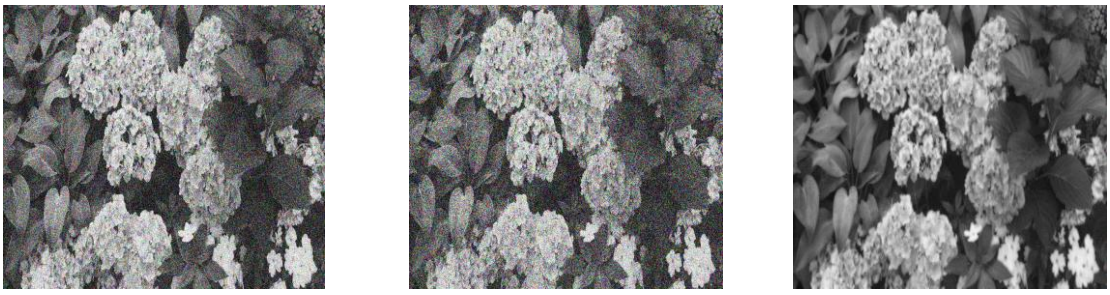

(a)Impulse noise (b)Effect drawing of mean filtering (c)Effect drawing of median filter

Figure 2. Denoising effect of median and mean filtering on impulse noise

Through experimental comparison, we can see that the intermediate filter can accurately capture the details and information of image edge when extracting noise. It is found in the image that the image is seriously damaged.

(3) Gaussian filter

Gaussian filtering algorithm has a positive impact on Gaussian noise emission. Gaussian filter function [11]: take the pixel density in the pixel region as the estimated value of the pixel. The pixel size decreases as the distance from the central pixel increases, indicating that the pixel plays a small role in pixel resolution. The size of Gaussian filter can be as shown in formula 2:

$$r(x,y)=\frac{1}{2\pi\sigma^2}e^{-\frac{x^2+y^2}{2\sigma^2}} \tag{2}$$

Among them, the sum of squares of X and Y represents the distance from the neighborhood pixel to the center point in the image. Parameter σ controls the smoothing degree of Gaussian filter on the image. The greater the value of σ, the greater the smoothing degree. On the contrary, the smoothing decline can not achieve the purpose of denoising.

(4) Bilateral filtering

The algorithm of bilateral filtering is simple and non iterative [12]. The principle expression is shown in equation 3:

$$f(x,y)=\frac{\sum_{(i,j)\subset D_{x,y}} F_s(i,j)F_r(i,j)\hat{f}(i,j)}{\sum_{(i,j)\subset D_{x,y}} F_s(i,j)F_r(i,j)} \tag{3}$$

Where, $f(x,y)$ represents the denoised image, D_{xy} represents the coordinate set of pixels in the neighborhood centered on point (x, y), $\hat{f}(i,j)$ represents the gray value of point (I, J) in the noisy image, and $F_s(i,j)$、$F_r(i,j)$ represents the spatial proximity weight and gray similarity weight between pixels in the neighborhood and central pixels respectively. σ_s、σ_r represents the filtering parameters [13].

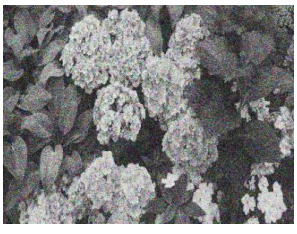

(a)Mean filtering diagram

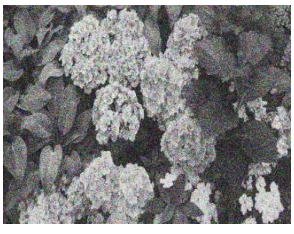

(b)Gaussian filter graph

(c)Bilateral filtering diagram

Figure 3. Gaussian noise image processing with different filters

In Fig. 3, three classical algorithms are used to process images containing Gaussian noise. It can be seen from the figure that the mean filtering does not filter the noise in the image, but weakens the noise points, which does not achieve the purpose of filtering the noise. Gaussian filtering blurs the image and loses the detailed information of the image while filtering out the noise [14]. While bilateral filtering can remove noise while preserving edge and detail information, there is still a serious problem of image detail loss. The nonlocal mean denoising algorithm effectively improves the shortcomings of the classical algorithm.

2.2. Sem Image Enhancement Algorithm

Due to the influence of image material or collection area, the original image quality will be very poor. In this case, the image will lose useful information and will be promoted due to unnecessary information. The purpose of image preview is to improve the image quality as needed, highlight the objects of interest through the modification process, and reduce or minimize unwanted objects and error messages [15]. Through image preview, we can improve the original data information and provide an important basis for displaying image features in the whole production process.

Image enhancement includes denoising, image enhancement, edge extraction and so on. Common systems include gray image conversion, histogram correction, image size adjustment, image density enhancement and other development technologies. The image resolution obtained by SEM is very high, and the application can capture the details of the process of applying ferroelectric thin films to high-resolution images. The image must be prefabricated and refined to reflect the physical properties and edge properties of ferroelectric materials [16].

Enhancement algorithm: image features often include the difference between the object and the back, the edge and contour of the object, etc. Improving the image can customize or enlarge these features to make the objects in the image better. After analysis, it is easy to deal with. For some original images that have been damaged or damaged by the test object, selecting the correct enhancement method can effectively eliminate the image noise and improve the edge or shape of the material [17]. Image enhancement changes the image effect of the image, but does not randomly generate image data, which can make the object features easier to identify. In this study, the initially proposed image enhancement methods include fuzzy positive methods based on fuzzy system, color coding and morphology to find the best image enhancement technology for different original SEM images.

The original image to be processed is represented by f, any pixel on f is represented by (m, n), and the gray level of this point is represented by k. If the original image is processed by the processing method t, the processed image is represented by g. If the gray scale of pixel (m, n) on g is represented by k ', then [18]:

$$k' = g(m,n) = t(k) \tag{4}$$

$$f = g(m,n) \tag{5}$$

1) Fuzzy set enhancement: the reason why image processing can play an important role in image processing is that all images have the loss of image information, which makes the image blurred, more or less blurred. The process of fuzzy set theory provides a scientific basis for locating confusion events through fuzzy thinking. The combination of fuzzy mathematics and image enhancement technology provides a new image enhancement method and idea, that is, the image enhancement method based on fuzzy system. This method first modifies the data of the original image according to the given group relative to the illusion area, then improves it according to the

conversion function, and finally achieves the improvement result by reverse mutation. The specific steps are shown in Fig. 4 [20].

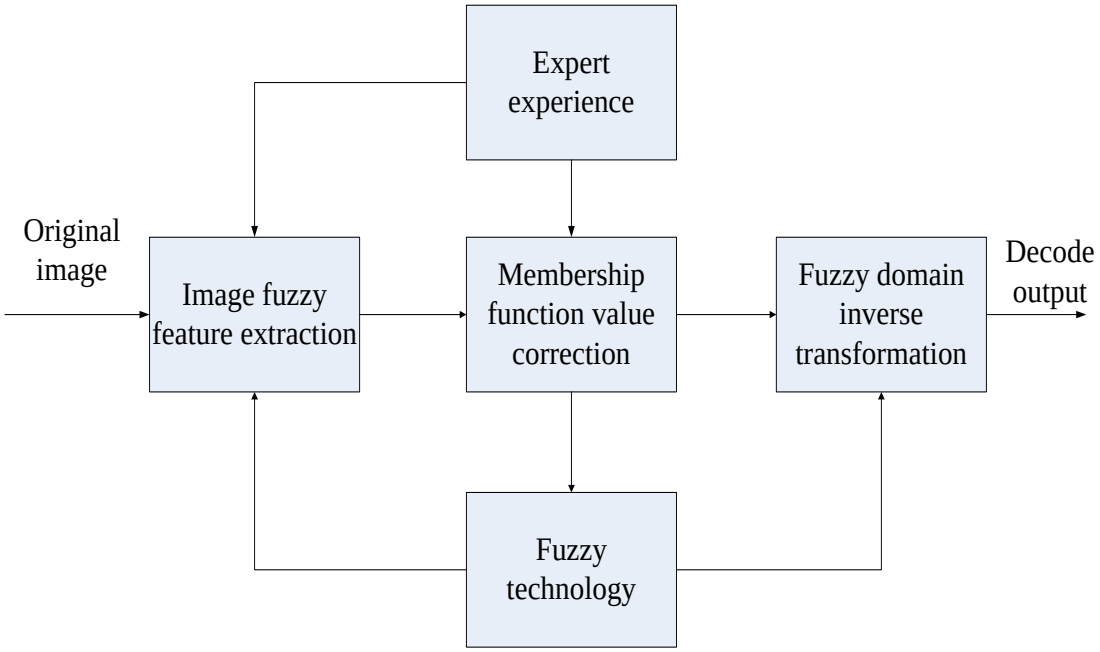

Figure 4. Steps of image enhancement based on fuzzy set

The theory treats the two-dimensional image as a fuzzy pixel set, which is expressed as:

$$S = \begin{bmatrix} \frac{p_{11}}{S_{11}} & \frac{p_{12}}{S_{12}} & \cdots & \frac{p_{1N}}{S_{1N}} \\ \frac{p_{21}}{S_{21}} & \frac{p_{22}}{S_{22}} & \cdots & \frac{p_{2N}}{S_{2N}} \\ \cdots & \cdots & \cdots & \cdots \\ \frac{p_{M1}}{S_{M1}} & \frac{p_{M2}}{S_{M2}} & \cdots & \frac{p_{MN}}{S_{MN}} \end{bmatrix} \tag{6}$$

In the above formula, S_{ij} represents the gray value of pixel points (i, j), p_{ij} represents pixel points (i, j), and $p_{ij} \in [0,1]$, the elements in these matrices represent the ratio of pixel gray in the original image to a set gray, which is called membership. Next, the fuzzy distribution of the data matrix needs to be solved by the algorithm, and the membership function is [21]:

$$\omega_{mn} = G(g_{mn}) = [1 + \frac{g_{\max} - g_j}{\mu_a}]^{-\mu_b} \tag{7}$$

In the above formula, $g_{\max}$ represents the maximum gray value of the pixel, and g_j represents the gray value of the current pixel. If there are $x_{ij} = S_c$ and $\omega_c = T(S_c) = 0.5$, then S_c is the crossing point. μ_a is called derivative fuzzy factor and μ_b is exponential fuzzy factor. These two parameters are determined by S_c generally, μ_b = 2 and μ_a is determined by formula [22]:

$$\mu_a = \frac{g_{\max} - g_j}{2^{\frac{1}{\mu_b}} - 1} \tag{8}$$

In order to correct the membership, the following transformation is adopted:

$$\omega_j = T_r(\omega_j) = T_w(T_{r-1}(\omega_j)) \qquad r = 1,2,3,\cdots \tag{9}$$

$$T(\omega_j) = \begin{cases} 2\cdot[\omega_j]^2 & 0 \le \omega_j \le 0.5 \\ 1-2\cdot[1-\omega_j]^2 & 0.5 \le \omega_j \le 1 \end{cases} \tag{10}$$

The above formula is the core step of image fuzzy enhancement. This formula shows that the key of fuzzy enhancement algorithm is to expand the membership gap. The specific implementation method is that when the membership value is greater than 0.5, it is increased by fuzzy enhancement operator, while the membership value less than 0.5 is reduced by operator [23]. After processing, the new feature plane will continuously enhance the image, and then the inverse transformation of membership degree is required. The inverse transformation equation is as follows [24]:

$$g_j^{'} = G^{-1}(\omega_j^{'}) = g_j - \mu_a[(\omega_j^{'})^{\frac{-1}{\mu_b}} - 1] \tag{11}$$

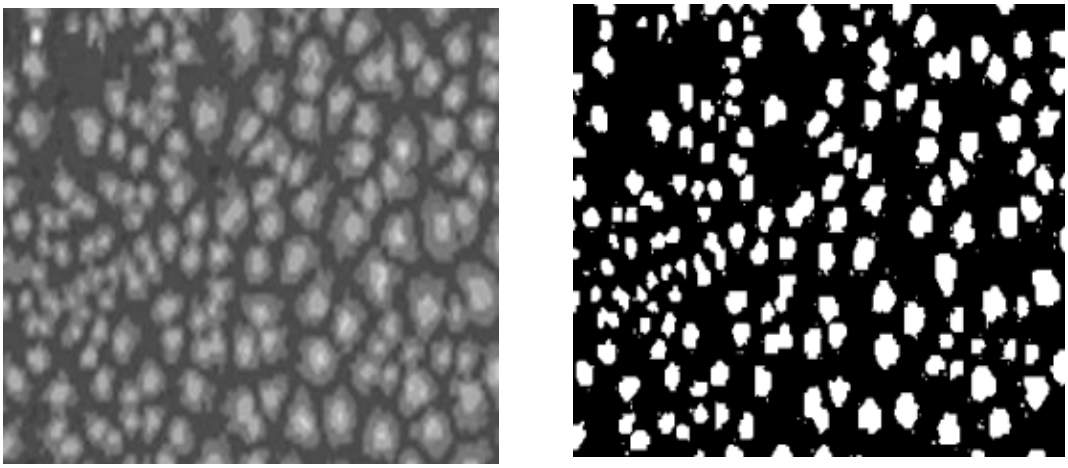

(a)SEM image of polysilicon film

(b)Fuzzy enhancement effect drawing

Figure 5. Fuzzy enhancement effect

Fig. 5 shows the results of synthesizing SEM images according to the fuzzy enhancement

method. Figure (a) is an SEM image of the prepared polysilicon film. The image is a crystalline mineral, and image (b) is the result of enhancement method based on fuzzy set. In comparison with the original image, it can be seen that the clarity has been significantly improved [25].

2) Pseudo color enhancement

Although the ferroelectric model obtained by SEM is a real 3D color image, the image only contains gray color, which is the same as the two-dimensional gray image, so only size information can be drawn [26]. When people look at the SEM images of ferroelectric materials, they often find many small differences in gray information that can not be seen by the naked eye. Sometimes these small differences are very useful for image detectors or important information. In order to distinguish these small differences, it can be considered to add color changes to the gray value of SEM images containing only gray information.

The process of pseudo color correction is the same as that of coloring under hardware conditions. The conversion effect of the three RGB elements is input to the three electron guns, and the output elements are also integrated into the whole image, as shown in Fig. 6 [27].

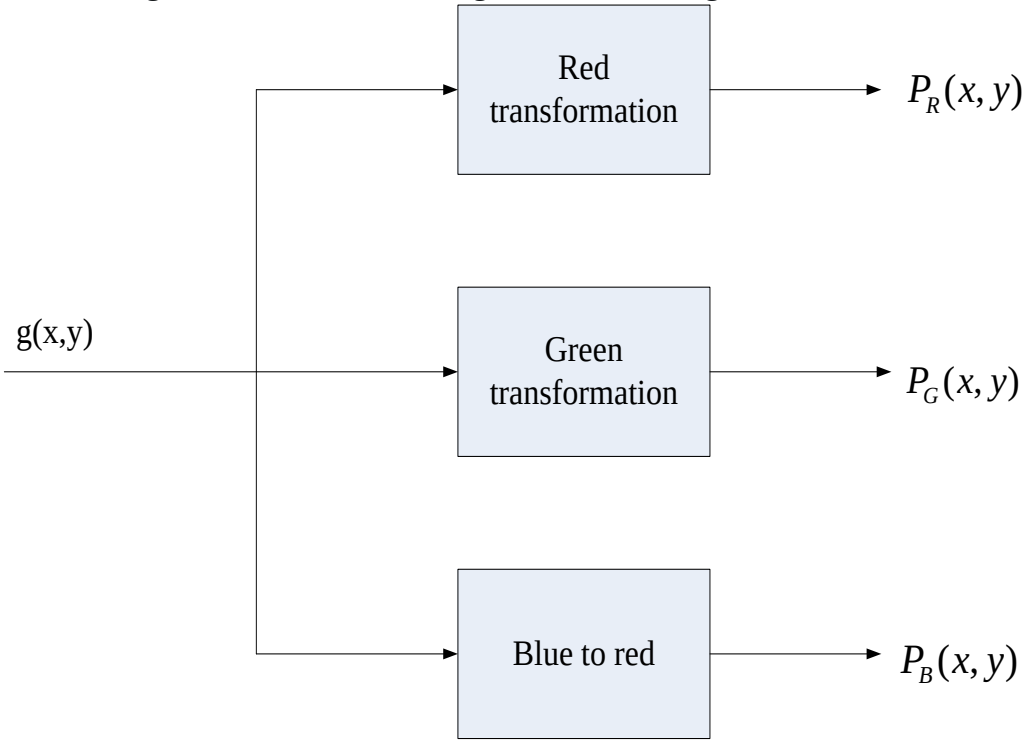

Figure 6. Pseudo color enhancement process

The mathematical expression of the process is as follows:

$$P(x,y) = (P_R(p(x,y)), P_G(p(x,y)), P_B(p(x,y))) \tag{12}$$

Among them, $p(x,y)$ represents the gray value of pixel (x, y), P_R、P_G、P_B represents the mapping relationship between pixel gray value and red, green and blue. This function is the core of converting pixels from gray to color, and the converted pixel color value $P(x,y)$ is composed of R, G and B [28].

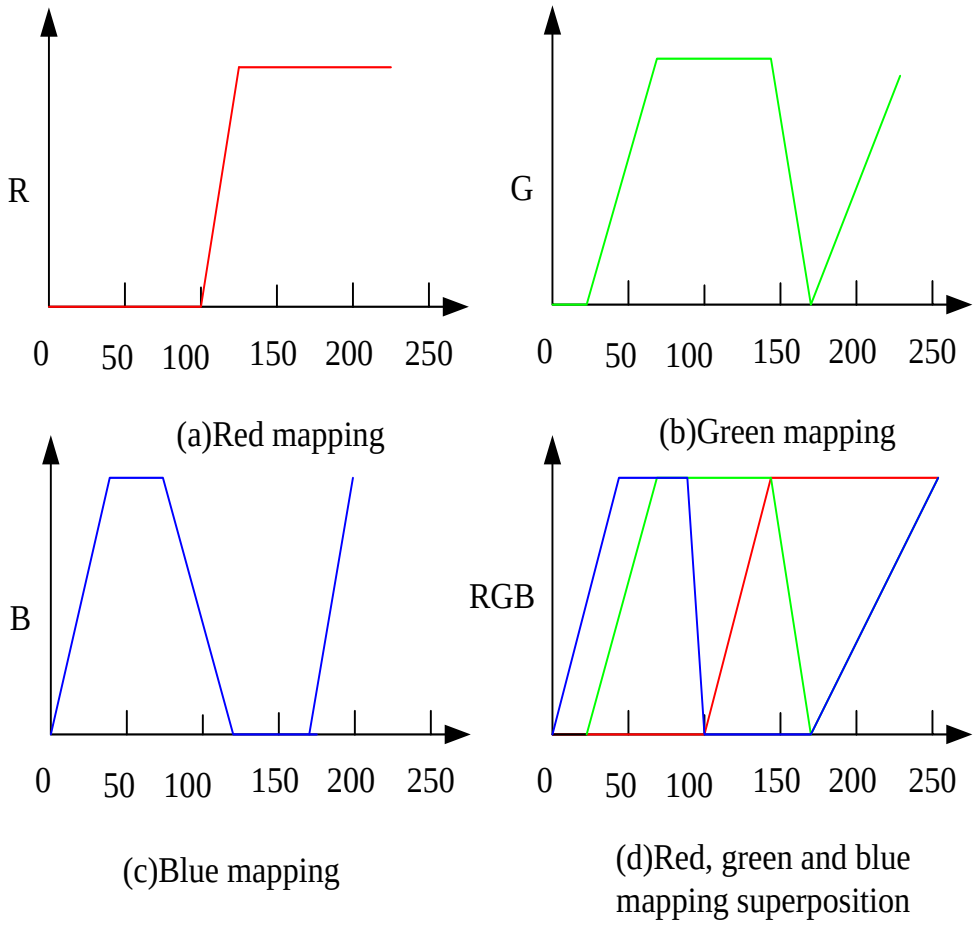

Figure 7. Rainbow encoding conversion curve

Rainbow coding is a common color coding algorithm. The conversion curve is shown in Figure 7. Figure (a) shows the mapping transformation between red and gray, and figures (b) and (c) show the mapping transformation between green and blue, respectively. Color image conversion and image (d) display three changes and are displayed in one coordinate.

In the SEM images with pseudo images, in order to further study the structural characteristics of materials, we must first eliminate its interference and combine the gray methods to achieve the ideal effect. For SEM nano silicon images containing false airflow images, although pseudo color enhancement enhances the morphology and position of ferroelectric materials, and distinguishes ferroelectric materials from airflow images by color, its purpose cannot be further discussed. In image processing, ferroelectric materials need to be separated from the substrate.

Mathematical morphology is abbreviated as morphology. Its design is based on mathematical geometry and mainly includes two basic elements: structural elements and physiological functions. When using morphology for image analysis, we must first select the correct components according to the characteristics of the object. On MATLAB, the syntax system is defined as SE = Strel (shape, parameters), where shape is a shape parameter, which is often used with rectangle, straight line, diamond, circle, etc. The parameters parameter refers to the size. The parameter representing its element dimension is in pixels. It can be seen that the changes of these two parameters will affect

the image processing effect. In practical application, the spacing of structural elements needs to be determined according to the characteristics of ferroelectric materials.

Ferroelectric memory is recognized as one of the most promising next-generation memories by society due to some advantages, such as high readability and writing speed, low power consumption, low charging and development resistance [29]. Among many ferroelectric materials, PZT thin film has always been a test point in the field of ferroelectric memory because of its residual polarization. However, the PZT film making temperature is too high, which will affect the compatibility and service life of the machine. Therefore, it is the main research direction to take some measures to reduce the preparation temperature of PZT films without affecting the electrical properties of the films.

The preparation process of PZT ferroelectric thin film is shown in Fig. 8 [30].

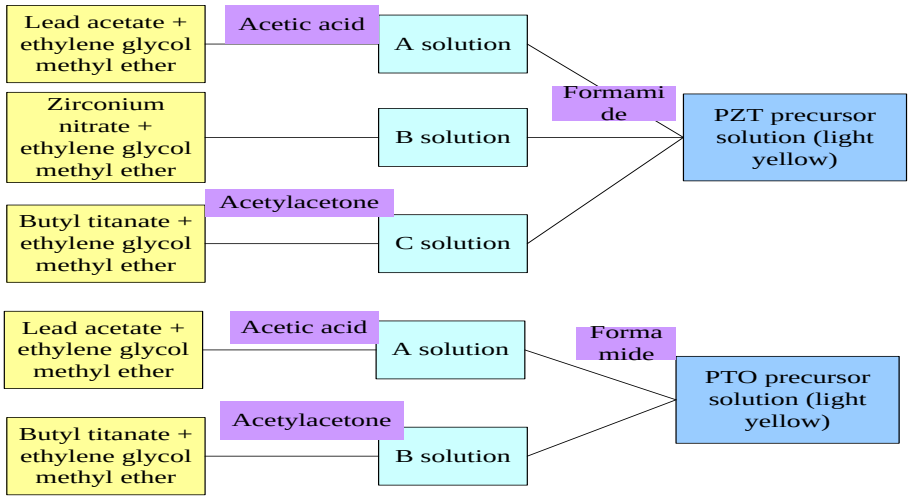

Figure 8. Preparation process diagram of PZT and PTO precursor solution

3. SEM Images Based on Denoising Algorithm Show the Effect of PTO Seed Layer on Crystallization Temperature and Electrical Properties of Pzt Ferroelectric Thin Films

In this experiment, sol-gel method was used to prepare $Pb(Zr_{0.52}Ti_{0.48})O_3$ (PZT) and $Pb(Zr_{0.52}Ti_{0.48})O_3 / PbTiO_3$ (PZT / PTO) ferroelectric thin films. In order to study the effect of seed layer on the microstructure of PZT films, we analyzed the SEM images of PZT and PZT / PTO films. The SEM images of the two films show smooth and complete morphology. As can be seen from Fig. 9 (a), the surface grain boundary of thin iron PZT film is clear, and the grain is large and uneven. At the same time, a small amount of pyrochlore can be seen in the film. As shown in Fig. 9 (b), it can be clearly seen from the cross-sectional view that grains and grain boundaries can be seen in some areas, and the screen is not dense enough. After adding PTO seed layer, the microstructure of PZT film changed significantly. PZT / PTO film has high surface density. The above results show that the addition of PTO seed layer is of great significance to improve the density of PZT films and promote the crystallization of PZT films.

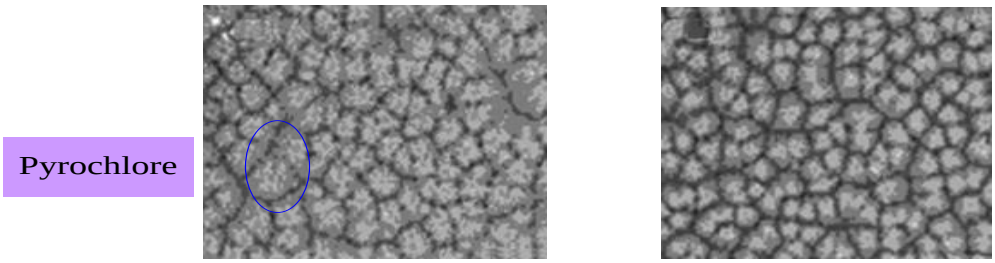

Figure 9. SEM images of PZT and PZT / PTO films

4. Comparative Study on Electrical Properties of PZT Films

In the case of electrical performance test, the indirect test is essentially to measure the hysteresis of the electrical circuit at different temperatures, and then use Maxwell's theory combined with the change of electric field to realize the temperature change under adiabatic conditions. The direct test method uses scanning calorimeter and thermal infrared camera to directly measure the temperature change. Table 1 shows the research results of some experimental electrical performance tests. Generally speaking, thin film materials or low-density materials have excellent electrical properties, which will be better than bulk materials or ceramic materials.

Table 1. Experimental research results of electrical properties

Material Science	$BaTiO_3$ ceramics	$Pb(Zr_{0.52}Ti_{0.48})O_3$	PMN-PT 65/35 film	(VDF-TrFE-CFE) 56.2/36.3/7.6 polymer film	PMN-PT 72/28 single crystal block
Temperature T(℃)	140	50	150	150	160
Temperature variationΔT(K)	6.0	9	31	42	3.3
Electric field changeΔE(MV/m)	1.2	6	54	70	1.0
$\Delta T/\Delta E(10^{-6}mV/K)$	5	1.5	0.57	0.6	3.3
Test method	Indirect test	Direct test	Indirect test	Indirect test	Indirect test

4.1. Ferroelectric Properties

Figure 10 (a) shows the hysteresis loops of two ferroelectric films PZT and PZT / PTO at different annealing temperatures. When the annealing temperature is about $650^{o}C$ and the voltage is 2.5 V, the residual polarization of PZT film is about $19\mu C/cm^{2}$ and the forced electric field is 60 kV / cm. After adding PTO seed layer, the residual polarization and cutting point of PZT film at the base do not change with the increase of annealing temperature, but only the complete polarization increases. In addition, it can be seen from the figure that when the PTO seed layer is added to the film, the residual polarization intensity obtained by annealing at $550^{o}C$ is about $20\mu C/cm^{2}$, which reduces the crystallization temperature of PZT film by about $100^{o}C$. Therefore, the ferroelectric properties of PZT films can be improved by adding PTO seed layer.

4.2. Dielectric Properties

Fig. 10 (b) is the correlation coefficient of dielectric measurement characteristics of PZT and PZT / PTO films after annealing $600^{o}C$, showing the variation trend of dielectric properties and dielectric loss with frequency at room temperature. As can be seen from the figure, initially, the dielectric values of the two PZT films further decreased with the increase of frequency. After 10^{6} Hz, it gradually increased. It can be clearly seen that the dielectric frequency of PZT / PTO film is higher than that of PZT film, and the dielectric loss is lower than that of PZT film. It can be seen from the SEM image that the low dielectric balance and high dielectric loss of PZT film are due to the low density of PZT / PTO film.

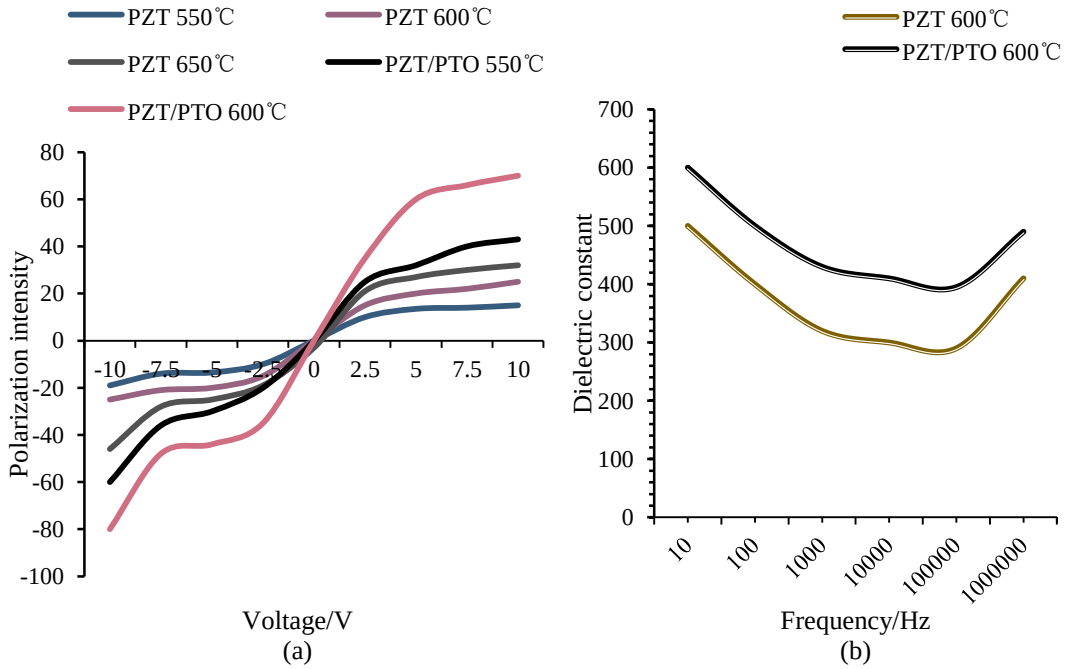

Figure 10. Electrical properties of PZT and PZT / PTO films at different temperatures

5. Conclusion

In this paper, the effects of adding PTO seed layer on the microstructure and electrical properties of ferroelectric PZT films were studied. After adding PTO seed layer, the SEM image of PZT film looks more compact and the crystallinity of the film is better. At the same time, the dense microstructure and grain distribution reduce the crystallization temperature of the film. Therefore, the maximum density of PZT / PTO film at 550 ℃ is the same as that of PZT iron film at 650 ℃. PZT / PTO films also achieve high dielectric frequency and low dielectric loss. Due to time reasons, the research of this paper is not deep enough, the scope involved is relatively small, and there are still many deficiencies to be improved.

Funding

This article is not supported by any foundation.

Data Availability

Data sharing is not applicable to this article as no new data were created or analysed in this study.

Conflict of Interest

The author states that this article has no conflict of interest.

References

[1] Chaudhary N, Savari S A. Increasing the Utilization of Deep Neural Networks for SEM Measurements Through Multiple Task Formulation and Visualization. IEEE Transactions on Semiconductor Manufacturing, 2020, PP(99):1-1.

[2] Huang X, Feng M, Gao C. Influence of P doping on transparent conductive property of SnO2:P thin film. Journal of Materials Science Materials in Electronics, 2017, 28(11):7593-7599.

[3] Basu N, Konduri A K, Basu P K, et al. Flexible, Label-Free DNA Sensor using Platinum oxide as the sensing element. IEEE Sensors Journal, 2017, PP(19):1-1.

[4] Boettger U, Waser R. Interaction between depolarization effects, interface layer, and fatigue behavior in PZT thin film capacitors. Journal of Applied Physics, 2017, 122(2):4002-1324. https://doi.org/10.1063/1.4992812

[5] Ren C, Tan C, Gong L, et al. Highly transparent, all-oxide, heteroepitaxy ferroelectric thin film for flexible electronic devices. Applied Surface Science, 2018, 458(NOV.15):540-545.

[6] Chen X, Qiao X, Zhang L, et al. Temperature dependence of ferroelectricity and domain switching behavior in Pb(Zr0 3Ti0.7)O3 ferroelectric thin films. Ceramics International, 2019, 45(14):18030-18036. https://doi.org/10.1016/j.ceramint.2019.06.022

[7] Lee M B. Structural and Ferroelectric Properties of PZT Thin Films Deposited on SrRuO 3 Electrode Films. Journal of the Korean Institute of Electrical and Electronic Material Engineers, 2016, 29(10):620-624. https://doi.org/10.4313/JKEM.2016.29.10.620

[8] Minh D H, Loi N V, Duc N H, et al. Low- temperature PZT thin-film ferroelectric memories fabricated on SiO2/Si and glass substrates. Journal of Science Advanced Materials & Devices, 2016, 1(1):75-79. https://doi.org/10.1016/j.jsamd.2016.03.004

[9] Ghasemzadeh H, Arjmandi M K. Universal audio steganalysis based on calibration and reversed frequency resolution of human auditory system. Iet Signal Processing, 2017, 11(8):916-922. https://doi.org/10.1049/iet-spr.2016.0690

[10] Mehranian A, Reader A J. Model-Based Deep Learning PET Image Reconstruction Using Forward-Backward Splitting Expectation Maximisation. IEEE Transactions on Radiation and Plasma Medical Sciences, 2020, PP(99):1-1.

[11] Zhuang F, Yi X, Tang L. An Adaptive Boosting Algorithm for Image Denoising. Mathematical Problems in Engineering, 2019, 2019(3):1-14. https://doi.org/10.1155/2019/8365932

[12] Gong Z, Chen B K, Liu J, et al. Robotic Probing of Nanostructures inside Scanning Electron Microscopy. IEEE Transactions on Robotics, 2017, 30(3):758-765. https://doi.org/10.1109/TRO.2014.2298551

[13] Park M R, Lee S G, Kim K M, et al. The ferroelectric properties of Ce-doped PZT/BFO multilayer thin films prepared using the sol-gel method. Journal of Ceramic Processing Research, 2017, 18(6):431-434.

[14] B, Satish, A, et al. Structural and electrical properties of pulsed laser deposited BaPbO3 conductive thin films and its effect on the ferroelectric properties of PbZr0.52Ti0.48O3 /BaPbO3 heterostructures. Ferroelectrics, 2017, 510(1):71-79.

[15] Desfeux R, Legrand C, Costa A D, et al. Correlation between local hysteresis and crystallite orientation in PZT thin films deposited on Si and MgO substrates. Surface ence, 2018, 600(1):219-228. https://doi.org/10.1016/j.susc.2005.09.053

[16] Lu G, Dong H, Chen J, et al. Enhanced dielectric and ferroelectric properties of PZT thin films derived by an ethylene glycol modified sol–gel method. Journal of Sol-Gel Science and Technology, 2017, 82(2):1-6. https://doi.org/10.1007/s10971-017-4311-5

[17] Bai Y, Wang Z J, He B, et al. Enhancement of Polarization in Ferroelectric Films via the Incorporation of Gold Nanoparticles. Acs Omega, 2017, 2(12):9067-9073. https://doi.org/10.1021/acsomega.7b01626

[18] Wang J, Jiang G, Huang W, et al. Ferroelectric properties of Ag doped PbZr 0.53 Ti 0.47 O 3 thin film deposited by sol–gel process. Journal of Materials Science: Materials in Electronics, 2019, 30(3):2592-2599. https://doi.org/10.1007/s10854-018-0534-7

[19] Antony J A, D Rangappa, Dutta S. Double doping effect on ferroelectric and leakage current behavior of Pb(Zr0.52Ti0.48)O3 thin film. Ceramics International, 2019, 45(18):25027-25033.

[20] Mi X, Zhang Z, Zhang W, et al. Fabrication of low-resistance LaNi_xO_(3+δ) thin films for ferroelectric device electrodes. Journal of Rare Earths, 2018, v.36(08):58-63. https://doi.org/10.1016/j.jre.2018.04.003

[21] Lim K W, Peddigari M, Annapureddy V, et al. Energy storage characteristics of {001 oriented Pb(Zr 0.52 Ti 0.48)O 3 thin film grown by chemical solution deposition. Thin Solid Films, 2018, 660(AUG.30):434-438. https://doi.org/10.1016/j.tsf.2018.04.041

[22] Sappati K K, Bhadra S. Flexible Piezoelectric 0–3 PZT-PDMS Thin Film for Tactile Sensing. IEEE Sensors Journal, 2020, 20(9):4610-4617.

[23] Gong D, Qin F, Wang Y, et al. Adjustable response of PZT thin film based piezoelectric micro-actuator through DC bias pre-polarization. Solid-State Electronics, 2020, 163(Jan.):107675.1-107675.7. https://doi.org/10.1016/j.sse.2019.107675

[24] MD Nguyen. Impact of fatigue behavior on energy storage performance in dielectric thin-film capacitors. Journal of the European Ceramic Society, 2020, 40(5):1886-1895.

[25] Shkuratov S I, Baird J, Antipov A G, et al. Stress-induced depolarization of single-layer PZT 95/5 ferroelectric films. Applied Physics Letters, 2019, 114(17):172902.1-172902.5.

https://doi.org/10.1063/1.5092632

[26] Yu B, Zhan J W, Yan N C, et al. Resistive Switching and Modulation of Pb(Zr0.4Ti0.6)O3/Nb:SrTiO3 Heterostructures. ACS Applied Materials And Interfaces, 2016, 8(48):32948-32955.

[27] Wang X W, Sun L Y, Wang X E, et al. A facile hot plate annealing at low temperature of Pb(Zr0.52Ti0.48)O3 thin films by sol–gel method and their ferroelectric properties. Journal of Materials Science: Materials in Electronics, 2018, 29(7):5660-5667.

[28] Brewer, S, J, et al. Enhanced radiation tolerance in Mn-doped ferroelectric thin films.. Applied Physics Letters, 2017, 111(2):1-5. https://doi.org/10.1063/1.4992791

[29] Junhwi, Lim, Y, et al. Optical evidence for the effect of gamma-ray irradiation on ferroelectric Pb(Zr0.52Ti0.48)O3 thin films. Journal of the Korean Physical Society, 2016, 68(11):1347-1351. https://doi.org/10.3938/jkps.68.1347

[30] Vandana, Gupta R, Tomar M, et al. Impact of TiO2 buffer layer on the ferroelectric photovoltaic response of CSD grown PZT thick films. Applied Physics A, 2021, 127(6):1-9. https://doi.org/10.1007/s00339-021-04552-3